

Supporting Information for:

# Ion-Specific Long-Range Correlations on Interfacial Water Driven by Hydrogen Bond Fluctuations

**Shinichi Enami\***

*The Hakubi Center for Advanced Research, Kyoto University, Kyoto 606-8302, Japan  
Research Institute for Sustainable Humanosphere, Kyoto University, Uji 611-0011, Japan  
PRESTO, Japan Science and Technology Agency, Kawaguchi 332-0012, Japan*

**Agustín J. Colussi\***

*Linde Center for Global Environmental Science, California Institute of Technology,  
California 91125, U.S.A*

## SI Text

In our experiments we measure (*in situ*, via online electrospray mass spectrometry, ES-MS, Kyoto University) relative anion populations,  $\chi = P_{127}/P_{79+81} = [I^-]/[Br^-]$ , in the water ‘films’ produced upon blowing up drops of sodium salt solutions by a high-speed gas as a function of ion additions in the 0.1 – 10  $\mu\text{M}$  range. Here we summarize the key mechanisms that give rise to mass spectral signals. Liquid solutions (injected as jets into the spraying chamber of the mass spectrometer) are sheared into primary drops by means of a co-directional high-speed nebulizer gas. Fig. S1 shows a schematic diagram of the initial droplet breakup. These primary drops are flattened by the moving gas, and then suddenly stretched windward into rimmed thin-film bags.<sup>1,2</sup> Given that the proximity of dissolved ions to the air-liquid interface varies along the span of the films, ions having larger propensities for the interface (i.e., ion X in Fig. S1B) become naturally enriched in the thinner sections of the film. In this process, ions

having smaller propensities (i.e., ion Y in Fig. S1B) accumulate in the rim whereas ions having larger propensities preferentially distribute along the film. The rimmed bags are dynamically unstable and fragment within tens of microseconds into smaller, sub-micrometer-sized secondary droplets. As expected from the preceding analysis, in the case of neat water droplets, the finer droplets originating from the film are negatively charged because they contain excess anions ( $\text{OH}^-$ ), whereas the coarser ones arising from the rims carry net positive charge ( $\text{H}^+$ ). These mechanisms were experimentally confirmed by Zilch et al.<sup>3</sup> The enhanced surface and electrostatic energies of the polarized stretched films are drawn from the kinetic energy of the gas. Since the kinetic energy density of the gas can deform only primary drops of  $d \sim 1$  mm diameter,<sup>4,5</sup> the breakup of the bag into charged secondary droplets is the primordial, one-time event in which net charges (those detected by mass spectrometry) are created from the neutral inflowing solutions. Sub-micron ( $d < 1 \mu\text{m}$ ) secondary droplets are just swept by the gas and rapidly shrink via solvent evaporation (enhanced by their large surface/volume ratios) thereby crowding their excess charges.<sup>6,7</sup> The fact that the titration curves of carboxylic acids and trimethylammonium determined in this setup are identical with the ionization constants reported in the literature (i.e.,  $\text{pK}_a \sim 4.8$  and  $\sim 9.8$ , respectively) suggests that solvent evaporation is minimal prior to droplet breakup.<sup>8-10</sup> Sub-micrometer-sized droplets eventually become Rayleigh-unstable and undergo a cascade of Coulomb explosions whose outcome is the ejection of bare single ions to the gas-phase.<sup>6,7</sup> Note that Coulomb explosions, in contrast with the aerodynamic breakup of primary droplets described above, arise from repulsion among like-charges and therefore preserve the overall charges of the initial ensemble of (positively and) negatively charged secondary droplets. By electrically biasing the inlet

to the detection chamber of the mass spectrometer we can monitor ions of either charge. Gas-phase ions are then sorted out and detected by the online mass spectrometer. Note that typical values of ion diffusion coefficients,  $D \approx 2 \times 10^{-5} \text{ cm}^2 \text{ s}^{-1}$ , and representative film lifetimes,  $\tau \approx 10^{-5} \text{ s}$ , lead to estimated mean diffusive displacements:  $\lambda = (2D\tau)^{1/2} \sim 2 \times 10^{-5} \text{ cm}$ , that are comparable to the average thickness of the present microfilms, suggesting that diffusion would assist ions to achieve equilibration.

We have showed that (i) the relative anion abundances at air–water interface, i.e., the mass-spectral signal intensities, measured on aqueous droplets consisting of equimolar solutions of mixed salts follow a normal Hofmeister series (as expected at the air–water interface of < a few nm thickness and confirmed by other surface-sensitive techniques) and are specifically affected by cationic or anionic surfactants,<sup>11,12,11,12</sup> (ii) mass spectra of aqueous droplets exposed to reactive gases detect species necessarily produced at the gas–liquid interface rather than in bulk water.<sup>13-19</sup> Data analysis based on mass balances and the kinetic theory of gases suggest that the thickness of the interfacial layers sampled in these experiments is less than a few nm, most likely below 1 nm.<sup>9</sup> More compellingly, we recently showed that the depth of the interfacial layers sampled in our experiments is controllable as a function of nebulizer gas velocity  $v_g$ .<sup>2</sup> This observation is consistent with the droplet breakup mechanism shown above and previous reports by other researchers.<sup>3</sup> Under the present high  $v_g$  ( $\sim 230 \text{ m/s}$ ) condition, ions reside at topmost layers of the air-water interface are preferentially detected as mass signals. Further experimental details and validation tests could be found in elsewhere.<sup>1,2,14,18,20-22</sup>

Typical conditions in the present experiments were: drying N<sub>2</sub> gas flow rate: 13 L min<sup>-1</sup>; nebulizer gas inlet pressure: 3.4 atm; drying N<sub>2</sub> gas temperature: 300 °C; inlet voltage: + 3.5 kV relative to ground; fragmentor voltage value: 80 V. NaI (purity > 99.5 %), NaBr (> 99 %), NaClO<sub>4</sub>-H<sub>2</sub>O (> 98 %), methanol (> 99.8 %), 2-propanol (> 99.7 %) were purchased from Nacalai Tesque (Kyoto). All chemicals were used as received. All solutions were prepared in purified water (Resistivity  $\geq$  18.2 M $\Omega$  cm at 298 K) from a Millipore Milli-Q water purification system. All experiments were performed at 293  $\pm$  2 K.

## SI References

- (1) Enami, S.; Colussi, A. J. Long-Range Hofmeister Effects of Anionic and Cationic Amphiphiles. *J. Phys. Chem. B* **2013**, *117*, 6276-6281.
- (2) Enami, S.; Colussi, A. J. Long-Range Specific Ion-Ion Interactions in Hydrogen-Bonded Liquid Films. *J. Chem. Phys.* **2013**, *138*, 184706.
- (3) Zilch, L. W.; Maze, J. T.; Smith, J. W.; Ewing, G. E.; Jarrold, M. F. Charge Separation in the Aerodynamic Breakup of Micrometer-Sized Water Droplets. *J. Phys. Chem. A* **2008**, *112*, 13352-13363.
- (4) Theofanous, T. G.; Mitkin, V. V.; Ng, C. L.; Chang, C. H.; Deng, X.; Sushchikh, S. The Physics of Aerobreakup. Ii. Viscous Liquids. *Phys. Fluids* **2012**, *24*, 022104.
- (5) Pilch, M.; Erdman, C. A. Use of Breakup Time Data and Velocity History Data to Predict the Maximum Size of Stable Fragments for Acceleration-Induced Breakup of a Liquid-Drop. *Int. J. Multiphase Flow* **1987**, *13*, 741-757.
- (6) Iribarne, J. V.; Thomson, B. A. On the Evaporation of Small Ions from Charged Droplets. *J. Chem. Phys.* **1976**, *64*, 2287.
- (7) Nguyen, S.; Fenn, J. B. Gas-Phase Ions of Solute Species from Charged Droplets of Solutions. *Proc. Natl. Acad. Sci. U. S. A.* **2007**, *104*, 1111-1117.
- (8) Mishra, H.; Enami, S.; Nielsen, R. J.; Stewart, L. A.; Hoffmann, M. R.; Goddard, W. A.; Colussi, A. J. Bronsted Basicity of the Air-Water Interface. *Proc. Natl. Acad. Sci. U.S.A.* **2012**, *109*, 18679-18683.
- (9) Enami, S.; Hoffmann, M. R.; Colussi, A. J. Proton Availability at the Air/Water Interface. *J. Phys. Chem. Lett.* **2010**, *1*, 1599-1604.
- (10) Cheng, J.; Psillakis, E.; Hoffmann, M. R.; Colussi, A. J. Acid Dissociation Versus

Molecular Association of Perfluoroalkyl Oxoacids: Environmental Implications. *J. Phys. Chem. A* **2009**, *113*, 8152-8156.

(11) Cheng, J.; Hoffmann, M. R.; Colussi, A. J. Anion Fractionation and Reactivity at Air/Water:Methanol Interfaces. Implications for the Origin of Hofmeister Effects. *J. Phys. Chem. B* **2008**, *112*, 7157.

(12) Cheng, J.; Vecitis, C.; Hoffmann, M. R.; Colussi, A. J. Experimental Anions Affinities for the Air/Water Interface. *J. Phys. Chem. B* **2006**, *110*, 25598.

(13) Enami, S.; Hoffmann, M. R.; Colussi, A. J. Dry Deposition of Biogenic Terpenes Via Cationic Oligomerization on Environmental Aqueous Surfaces. *J. Phys. Chem. Lett.* **2012**, *3*, 3102-3108.

(14) Enami, S.; Stewart, L. A.; Hoffmann, M. R.; Colussi, A. J. Superacid Chemistry on Mildly Acidic Water. *J. Phys. Chem. Lett.* **2010**, *1*, 3488-3493.

(15) Enami, S.; Hoffmann, M. R.; Colussi, A. J. Prompt Formation of Organic Acids in Pulse Ozonation of Terpenes on Aqueous Surfaces. *J. Phys. Chem. Lett.* **2010**, *1*, 2374-2379.

(16) Enami, S.; Hoffmann, M. R.; Colussi, A. J. Ozonolysis of Uric Acid at the Air/Water Interface. *J. Phys. Chem. B* **2008**, *112*, 4153-4156.

(17) Enami, S.; Hoffmann, M. R.; Colussi, A. J. Acidity Enhances the Formation of a Persistent Ozonide at Aqueous Ascorbate/Ozone Gas Interfaces. *Proc. Natl. Acad. Sci. U. S. A.* **2008**, *105*, 7365-7369.

(18) Enami, S.; Vecitis, C. D.; Cheng, J.; Hoffmann, M. R.; Colussi, A. J. Electrospray Mass Spectrometric Detection of Products and Short-Lived Intermediates in Aqueous Aerosol Microdroplets Exposed to a Reactive Gas. *J. Phys. Chem. A* **2007**, *111*, 13032-13037.

(19) Enami, S.; Sakamoto, Y.; Colussi, A. J. Fenton Chemistry at Aqueous Interfaces. *Proc. Natl. Acad. Sci. U.S.A.* **2014**, *111*, 623-628.

(20) Enami, S.; Hoffmann, M. R.; Colussi, A. J. Molecular Control of Reactive Gas Uptake "on Water". *J. Phys. Chem. A* **2010**, *114*, 5817-5822.

(21) Enami, S.; Vecitis, C. D.; Cheng, J.; Hoffmann, M. R.; Colussi, A. J. Mass Spectrometry of Interfacial Layers During Fast Aqueous Aerosol/Ozone Gas Reactions of Atmospheric Interest. *Chem. Phys. Lett.* **2008**, *455*, 316-320.

(22) Enami, S.; Vecitis, C. D.; Cheng, J.; Hoffmann, M. R.; Colussi, A. J. Global Inorganic Source of Atmospheric Bromine. *J. Phys. Chem. A* **2007**, *111*, 8749-8752.

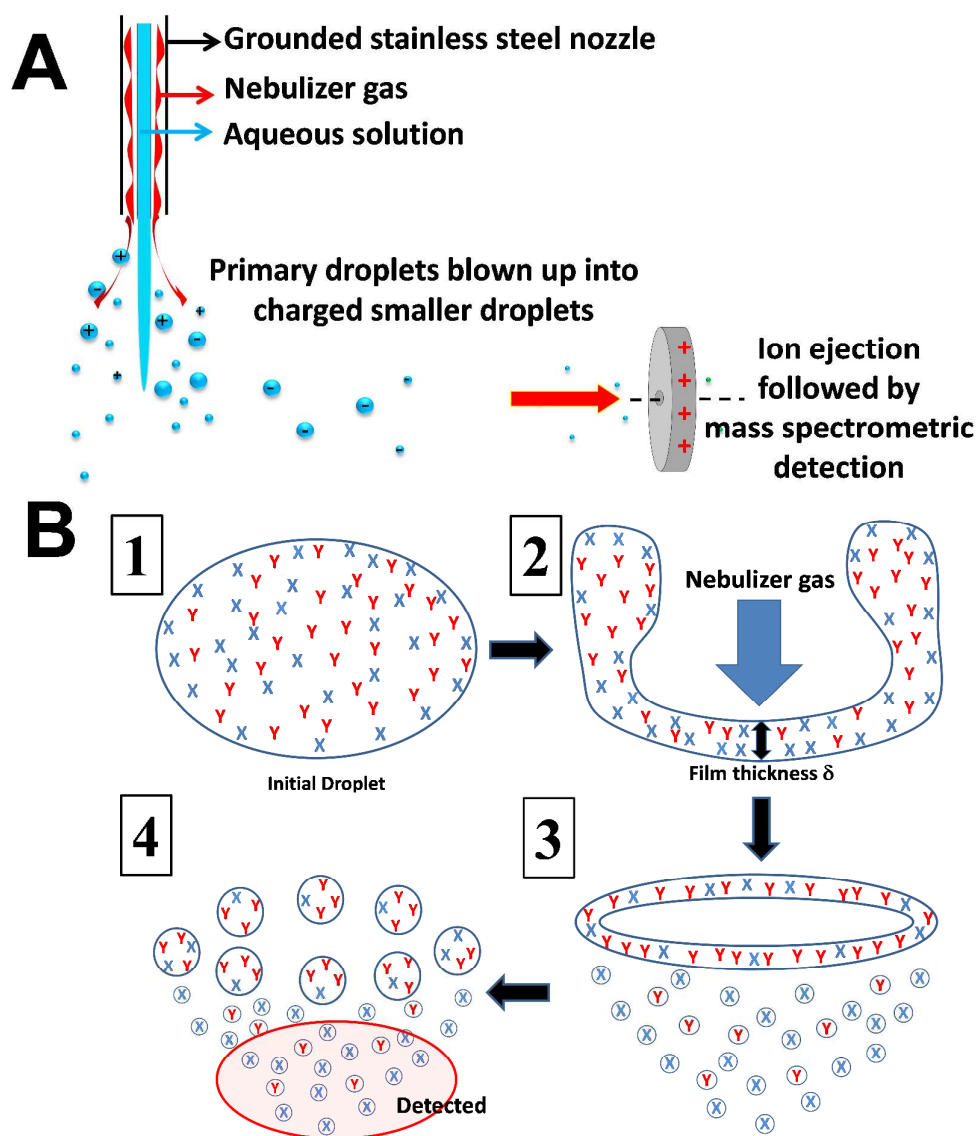


**Figure S1** A) Schematics of liquid injection, nebulization, droplet breakup and ion ejection and B) Schematic illustration of a droplet breakup mechanism.  $\delta$  is the thickness of the film. In our experiments we sample the anions contained in the sub-micrometer-droplets generated from the center of the film, which are detected *in situ* by online electrospray mass spectrometry. Anions having the largest propensities

for the air-liquid interface, such as  $\text{I}^-$  and  $\text{ClO}_4^-$ , produce the most intense mass signals.

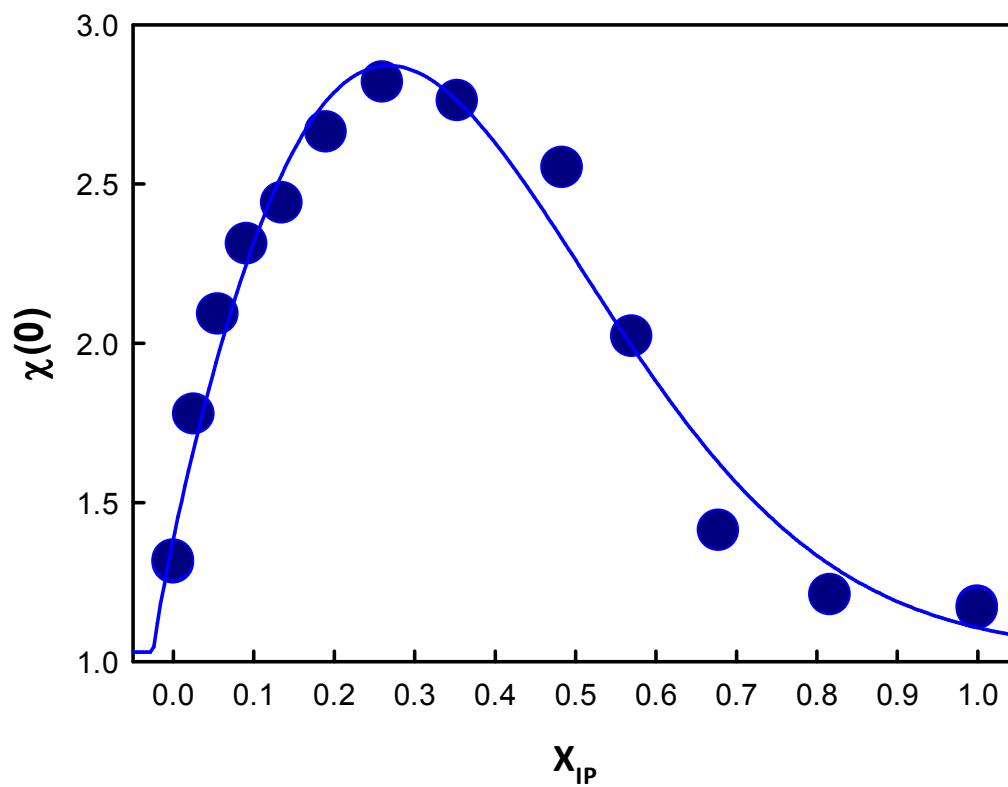


**Figure S2** Plots of the ratio  $\chi(0)$  of ES mass spectral signal intensities  $\chi = \text{I}^-/\text{Br}^-$  in films of (5  $\mu\text{M}$  NaI + 20  $\mu\text{M}$  NaBr) solutions in  $\text{H}_2\text{O}$ -IP mixture solvents as a function of molar fraction of IP,  $x_{\text{IP}}$ .